Redox Chemistry Associated with the Complexation of Vanadium(V) and Tungsten(VI) by *meso*-Octaethylporphyrinogen: Formation and Cleavage of Cyclopropane Units Functioning as Shuttles of Two Electrons

Umberto Piarulli,[1a] Euro Solari,[1a] Carlo Floriani,*,[1a] Angiola Chiesi-Villa,[1b] and Corrado Rizzoli[1b]

Contribution from the Institut de Chimie Minérale et Analytique, BCH, Université de Lausanne, CH-1015 Lausanne, Switzerland, and Dipartimento di Chimica, Università di Parma, I-43100 Parma, Italy

Received December 29, 1995[⊗]

Abstract: Oxidized forms of *meso*-octaethylporphyrinogen containing mono- and bis(cyclopropane) units, which function as shuttles of two electrons, form from the reaction of high-valent, early transition metal halides, namely [*p*-$MeC_6H_4N{\equiv}VCl_3$] (**2**) and $WOCl_4$, with *meso*-octaethylporphyrinogen−lithium derivatives, $[Et_8N_4Li_4(THF)_4]$ (**1**). The reaction of **2** with **1** occurs in a 2:1 ratio since the intermediate vanadium(V)−porphyrinogen complex undergoes a fast one-electron oxidation by **2** leading to [*p*-$MeC_6H_4N{\equiv}V\{Et_8N_4(\Delta)\}$] (**3**), which contains a vanadium(IV)−nitrene fragment bound to the two-electron, oxidized form of the porphyrinogen having a cyclopropane unit. This latter can be reduced using Li metal to a vanadium(IV)−porphyrinogen complex, [*p*-$MeC_6H_4N{\equiv}V(Et_8N_4)Li_2(THF)_4\}$] (**5**), which was also synthesized from **1** and [(*p*-$MeC_6H_4N{\equiv}VCl_2)_2$] (**4**). In the reaction of $WOCl_4$, we found that the tungsten(VI)−porphyrinogen complex forms first and is able to oxidize the excess of **1**, to give $[Et_8N_4(\Delta)Li_2(THF)_2]$ (**8**) or the $[Et_8N_4(\Delta)_2Li(THF)]^+$ cation (**9B**), depending on the stoichiometric ratio. The former forms along with $[Et_8N_4W{=}OLi(THF)_4]$ (**7**) when a $WOCl_4$:**1** ratio of 2:3 was used. In the case of a 4:5 ratio, **9B** was isolated as a countercation of $[Et_8N_4W{=}O]^-$ (**9A**). The bis(cyclopropane) form of porphyrinogen becomes available by reacting **9** with $NaBPh_4$, thus forming $[Et_8N_4(\Delta)_2Li]^+BPh_4^-$ (**11**). The lithium derivatives, **8** and **11**, are the oxidized forms of porphyrinogen available for synthesis. The tungstenyl anion in **7** can be converted into the inorganic ester $[Et_8N_4WOC(O)Ph]$ (**12**) by reacting it with PhCOCl.

Introduction

meso -Octaethylporphyrinogen[2,3] has a very peculiar redox chemistry associated with the formation and cleavage of cyclopropane units within the porphyrinogen skeleton.[4] This is due to the absence of any *meso*-hydrogen, which prevents the usual aromatization to porphyrin. Dealkylating aromatization, although much more difficult, has been observed in a few cases[5] (see Scheme 1). The cyclopropane units function as two electron shuttles being formed and reduced under very mild conditions. The formation of two cyclopropane moieties within the porphyrinogen skeleton can occur either by an intra- or an intermolecular redox process. It proceeds in two steps *via* monoelectronic exchange reactions. The metal-to-ligand synergism allows the assumption of the presence of the cyclopropane unit as a masked form of an additional +2 oxidation state for the metal.

Thus, the porphyrinogen has a self-controlling effect on the oxidation state of the metal, depending on whether the oxidized or reduced form binds the metal center. We report here how the complexation of high-valent, early transition metals is affected by the redox chemistry of the *meso*-octaethylporphyrinogen, allowing the existence of defined oxidation states of the metal and of the ligand. The metalation of *meso*-octaethylporphyrinogen with [$ArN{\equiv}VCl_3$] (Ar = *p*-MeC_6H_4) and $WOCl_4$ allows us to discover some unprecedented porphyrinogen complexes of early transition metals and the redox chemistry which is associated with them. It also led to the first applicable synthetic procedure for the oxidized forms of *meso*-octaethylporphyrinogen containing cyclopropane units.

* To whom correspondence should be addressed.

⊗ Abstract published in *Advance ACS Abstracts,* April 1, 1996.

(1) (a) Université de Lausanne. (b) Università di Parma.

(2) (a) Fischer, H.; Orth, H. *Die Chemie des Pyrrols;* Akademische Verlagsgesellschaft: Leipzig, Germany, 1934; p 20. (b) Dennstedt, M.; Zimmermann, J. *Chem. Ber.* **1887,** *20,* 850, 2449; **1888**, *21,* 1478. (c) Dennstedt, D. *Chem. Ber.* **1890**, *23,* 1370. (d) Chelintzev, V. V.; Tronov, B. V. *J. Russ. Phys. Chem. Soc.* **1916**, *48,* 105, 127. (e) Sabalitschka, Th.; Haase, H. *Arch. Pharm.* **1928**, *226,* 484. (f) Rothemund, P.; Gage, C. L. *J. Am. Chem. Soc.* **1955**, *77,* 3340.

(3) For references to metal complexation by *meso*-octaalkylporphyrinogen, see: (a) Jacoby, D.; Floriani, C.; Chiesi-Villa, A.; Rizzoli, C. *J. Chem. Soc., Chem. Commun.* **1991**, 220. (b) Jacoby, D.; Floriani, C.; Chiesi-Villa, A.; Rizzoli, C. *J. Chem. Soc., Chem. Commun.* **1991**, 790. (c) Jubb, J.; Jacoby, D.; Floriani, C.; Chiesi-Villa, A.; Rizzoli, C. *Inorg. Chem.* **1992**, *31,* 1306. (d) Jacoby, D.; Floriani, C.; Chiesi-Villa, A.; Rizzoli, C. *J. Am. Chem. Soc.* **1993**, *115,* 3595. (e) Jacoby, D.; Floriani, C.; Chiesi-Villa, A.; Rizzoli, C. *J. Am. Chem. Soc.* **1993**, *115,* 7025. (f) Rosa, A.; Ricciardi, G.; Rosi, M.; Sgamellotti, A.; Floriani, C. *J. Chem. Soc., Dalton Trans.* **1993**, 3759. (g) De Angelis, S.; Solari, E.; Floriani, C.; Chiesi-Villa, A.; Rizzoli, C. *J. Chem. Soc., Dalton Trans.* **1994**, 2467. (h) Jacoby, D.; Isoz, S.; Floriani, C.; Chiesi-Villa, A.; Rizzoli, C. *J. Am. Chem. Soc.* **1995**, *117,* 2793. (i) Jacoby, D.; Isoz, S.; Floriani, C.; Chiesi-Villa, A.; Rizzoli, C. *J. Am. Chem. Soc.* **1995**, *117,* 2805. (j) Floriani, C. In *Stereoselective Reactions of Metal-Activated Molecules;* Werner, H., Sundermeyer, J., Eds.; Vieweg: Wiesbaden, Germany, 1995; p 97. (k) De Angelis, S.; Solari, E.; Floriani, C.; Chiesi-Villa, A.; Rizzoli, C. *Angew. Chem., Int. Ed. Engl.* **1995**, *34,* 1092. (l) De Angelis, S.; Solari, E.; Floriani, C.; Chiesi-Villa, A.; Rizzoli, C. *Organometallics* **1995**, *14,* 4505. (m) Jacoby, D.; Isoz, S.; Floriani, C.; Chiesi-Villa, A.; Rizzoli, C. *Organometallics* **1995**, *14,* 4816.

(4) (a) De Angelis, S.; Solari, E.; Floriani, C.; Chiesi-Villa, A.; Rizzoli, C. *J. Am. Chem. Soc.* **1994**, *116,* 5691. (b) De Angelis, S.; Solari, E.; Floriani, C.; Chiesi-Villa, A.; Rizzoli, C. *J. Am. Chem. Soc.* **1994**, *116,* 5702. (c) Floriani, C. In *Transition Metals in Supramolecular Chemistry*; Fabbrizzi, L., Poggi, A., Eds.; Nato ASI Series; Kluwer: Dordrecht, The Netherlands, 1994; Vol. 448, pp 191−209.

(5) (a) Piarulli, U.; Floriani, C.; Chiesi-Villa, A.; Rizzoli, C. *J. Chem. Soc., Chem. Commun.* **1994**, 895. (b) Solari, E.; Musso, F.; Floriani, C.; Chiesi-Villa, A.; Rizzoli, C. *J. Chem. Soc., Dalton Trans.* **1994**, 2015.

0002-7863/96/1518-3634$12.00/0

Scheme 1

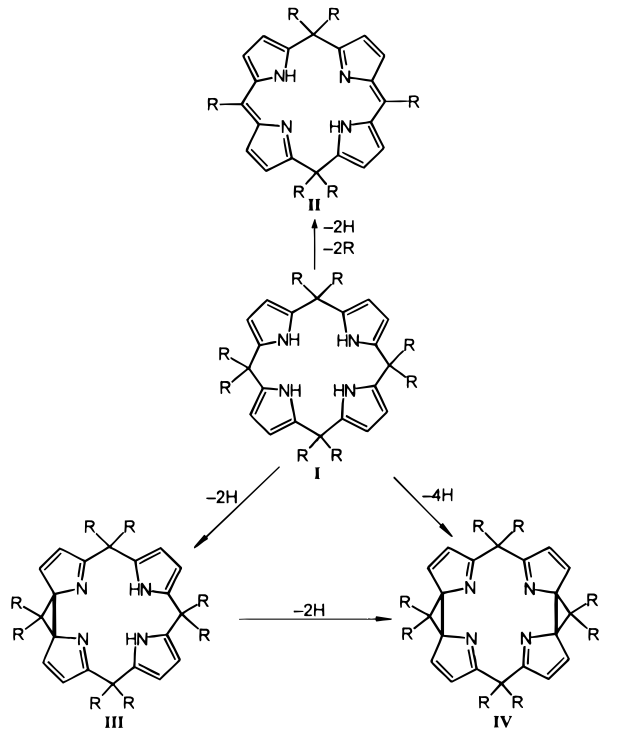

Scheme 2

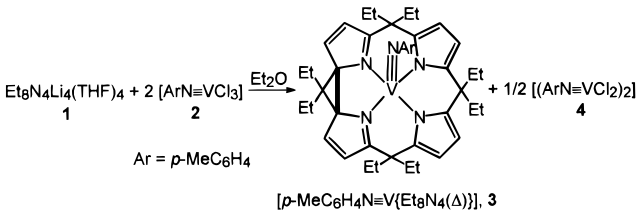

Results and Discussion

The complexation of metal ions by the *meso*-octaethylporphyrinogen ($Et_8N_4H_4$) has been carried out according to the procedure recently published in several papers.[3] This procedure requires the use of the lithiated form of porphyrinogen, [$Et_8N_4Li_4(THF)_4$], in nonaqueous solvents.[3g] The reaction of **1** with **2** was carried out in Et_2O. As a matter of fact, when the dimer **2** is dissolved in Et_2O, it is converted to a solvated monomer [p-$MeC_6H_4N{\equiv}VCl_3(Et_2O)_2$].[6] The same solid state−solution conversion is observed in THF. After a number of attempts, the stoichiometry was adjusted to the values reported in Scheme 2.

Although the separation of **3** and **4**[6] is a bit difficult due to their very close solubilities, both have been identified and **3** has been structurally characterized. Complex **3** has a magnetic moment of $\mu = 1.81\ \mu_B$, indicating the presence of a vanadium(IV).

Selected bond distances and angles for complexes **3** and **7**−**9** are listed in Table 1. Table 2 compares the most relevant conformational parameters for the four complexes; the pyrrole rings containing N1, N2, N3, and N4 are labeled A, B, C, and D, respectively. The labeling scheme adopted for the basic macrocycle ligand is in Figure 1.

The structure of **3** consists of discrete [$Et_8N_4(\Delta)V$(N-p-C_6H_4-Me)] complex molecules (Figure 2) (hereinafter the cyclopropane unit will be indicated by Δ). Coordination around vanadium is square pyramidal with the basal plane being provided by the N_4 core of the porphyrinogen and the apex by the nitrogen atom of the *p*-tolylimido ligand. The cation is displaced by 0.638(1) Å from the basal plane toward the N5 atom. The dihedral angle between the V−N5 line and the normal to the basal plane is 0.8(1)°, and the V1−N5−C37 angle is 173.5(2)°. The conformation of the macrocycle differs from those previously observed for porphyrinogen complexes containing a cyclopropane unit,[4] with the B, C, and D rings being tilted down and the A ring being tilted up with respect to the the N_4 plane. As typically observed for η^1-bonded pyrrole rings containing charged nitrogen atoms, the trend of the bond distances within the A and B rings is consistent with a partial C=C double bond localization on the carbon atoms adjacent to the macroring, the average value calculated for the C1−C2, C3−C4, C6−C7, and C8−C9 bond distances [1.373(2) Å] being slightly, but significantly, shorter than the average value calculated for the C2−C3 and C7−C8 bonds [1.403(2) Å]. The C and D rings bridged by the cyclopropane unit show a system of conjugated double bonds as indicated by the double-bond character of N3−C11, C12−C13, N4−C19, and C17−C18 and the single-bond character of N3−C14, C11−C12, C13−C14, N4−C16, C16−C17, and C18−C19. The configurations at the C14 and C16 asymmetric carbon atoms are *S* and *R*, respectively, with reference to the coordinates of Table S2. Since the space group is centrosymmetric, the enantiomeric diastereoisomer is present in the structure.

A few structural parameters within the coordination sphere of the metal should be mentioned: (i) the linearity of the V1−N5−C37 moiety [173.5(2)°] and the short V1−N5 distance associated with it [1.671(2) Å], which is similar to other vanadium−nitrene fragments occurring in organometallic chemistry;[6] (ii) the differences in the V−N distances within the macrocycle, with those involving the neutral nitrogen being significantly longer [V1−N3, 2.109(2), and V1−N4, 2.110(2) Å *vs* V1−N1, 2.021(2), and V1−N2, 2.055(2) Å]; (iii) the quite close geometrical proximity between the V≡N functionality and the hydrogen atoms of the methylene groups C31 and C35 [H311···V1, 2.84 Å; H311···N5, 2.46 Å; C31···N5, 3.457(3) Å; C31−H311···N5, 171°; H352···V1, 2.88 Å; H352···N5, 2.57 Å; C35···N5, 3.489(3) Å; C35−H352···N5, 166°]. The C31···C35 separation is 4.450(4) Å. This is an extremely significant contact, due to the special role that this functionality plays in the activation of hydrocarbons, including the addition of the C−H across a vanadium−nitrogen triple bond.[7]

The genesis of **3** is a consequence of the redox chemistry usually associated with metal−porphyrinogen complexes. In this particular case, we should admit that the porphyrinogen tetraanion has a high inclination to undergo oxidation by vanadium(V).

Thus the preliminary porphyrinogen complex **A** (Scheme 3) may be considered as more stable in the form of a vanadium(IV)−porphyrinogen, free radical species, which undergoes a one-electron oxidation in the presence of an excess of **2**, which is obviously supposed to react faster as an oxidant than in binding **1**. The diradical form, **C**, is formally a precursor of the cyclopropane moiety in **3**. The function of **2** as a monoelectronic oxidant is reminiscent of the action of "$CuCl_2$" we used in the formation of the oxidized form of porphyrinogen containing cyclopropane moieties.[4] In order to prove the incompatibility of the vanadium(V) with the porphyrinogen tetraanion, we tried to access complex **A** in Scheme 3 by the

(6) Solan, G.; Cozzi, P. G.; Floriani, C.; Chiesi-Villa, A.; Rizzoli, C. *Organometallics* **1994**, *13*, 2572 and references therein.

(7) (a) de With, J.; Horton, A. D. *Organometallics* **1990**, *9*, 2207. (b) de With, J.; Horton, A. D. *Organometallics* **1993**, *12*, 1493. (c) de With, J.; Horton, A. D. *Angew. Chem., Int. Ed. Engl.* **1993**, *32*, 903.

Table 1. Selected Interatomic Distances (Å) and Bond Angles (deg) for Complexes **3** and **7**−**9** (M = V for **3**; M = W for **7** and the Anion of **9**; M = Li1 for **3** and for the Cation of **9**)

				9						9	
	3	**7**	**8**	anion	cation		**3**	**7**	**8**	anion	cation
M−O1		1.732(8)		1.669(10)		C1−C2	1.373(3)	1.36(2)	1.378(3)	1.42(3)	1.49(3)
M−O2		2.401(8)	1.943(4)		2.01(3)	C1−C20	1.522(3)	1.51(2)	1.515(3)	1.49(3)	1.47(2)
M−N1	2.055(2)	2.080(8)	2.276(4)	2.055(12)	2.19(2)	C2−C3	1.406(3)	1.40(2)	1.416(3)	1.38(4)	1.39(3)
M−N2	2.021(2)	2.083(10)	2.325(4)	2.073(11)	2.16(3)	C3−C4	1.385(4)	1.37(2)	1.386(3)	1.36(3)	1.49(2)
M−N3	2.110(2)	2.110(8)	2.165(4)	2.046(11)	2.22(3)	C4−C5	1.514(2)	1.51(2)	1.524(3)	1.50(2)	1.52(3)
M−N4	2.109(2)	2.104(10)	2.225(4)	2.036(10)	2.23(3)	C4−C6	2.578(3)	2.55(2)	2.529(3)	2.47(2)	1.55(2)
M−N5	1.671(2)					C5−C6	1.519(3)	1.53(2)	1.530(3)	1.49(2)	1.52(3)
Li2−O1		1.90(2)				C6−C7	1.365(3)	1.36(2)	1.384(3)	1.36(2)	1.45(3)
Li2−O3		1.95(2)	1.903(4)			C7−C8	1.395(5)	1.39(2)	1.412(3)	1.41(3)	1.34(3)
Li2−O4		1.94(3)				C8−C9	1.372(3)	1.36(2)	1.377(3)	1.35(2)	1.49(3)
Li2−O5		1.94(2)				C9−C10	1.512(3)	1.49(2)	1.518(3)	1.49(2)	1.57(3)
Li2−N1			1.982(4)			C10−C11	1.503(2)	1.51(2)	1.513(3)	1.50(2)	1.51(2)
Li2−N2			1.969(4)			C11−C12	1.459(3)	1.38(2)	1.473(3)	1.31(2)	1.51(3)
N1−C1	1.388(3)	1.43(2)	1.380(3)	1.39(3)	1.32(2)	C12−C13	1.337(3)	1.41(2)	1.329(3)	1.41(2)	1.36(3)
N1−C4	1.380(3)	1.41(2)	1.381(3)	1.38(2)	1.42(2)	C13−C14	1.459(4)	1.37(2)	1.463(3)	1.42(2)	1.49(3)
N2−C6	1.395(3)	1.396(14)	1.385(3)	1.43(2)	1.48(2)	C14−C15	1.536(3)	1.51(2)	1.526(3)	1.51(2)	1.50(2)
N2−C9	1.392(3)	1.42(2)	1.379(3)	1.38(2)	1.24(2)	C14−C16	1.551(3)	2.53(2)	1.574(3)	2.47(2)	1.59(2)
N3−C11	1.309(3)	1.41(2)	1.301(3)	1.46(2)	1.29(2)	C15−C16	1.542(3)	1.50(2)	1.523(3)	1.38(3)	1.51(2)
N3−C14	1.449(2)	1.386(13)	1.431(3)	1.42(2)	1.40(2)	C16−C17	1.462(2)	1.37(2)	1.468(3)	1.40(2)	1.51(2)
N4−C16	1.441(3)	1.417(14)	1.440(3)	1.39(2)	1.40(2)	C17−C18	1.347(3)	1.44(2)	1.326(3)	1.41(3)	1.33(2)
N4−C19	1.302(3)	1.41(2)	1.305(3)	1.39(2)	1.30(2)	C18−C19	1.463(2)	1.34(2)	1.478(3)	1.37(2)	1.42(2)
N5−C37	1.375(3)					C19−C20	1.520(3)	1.51(2)	1.511(3)	1.53(3)	1.53(2)
N3−M−N4	76.6(1)	88.4(3)	76.2(1)	86.2(4)	76.3(8)	N2−C6−C5	123.6(2)	121.9(11)	120.4(2)	122.8(12)	119(2)
N2−M−N4	143.4(1)	159.9(4)	132.8(2)	146.7(4)	135.3(12)	N2−C6−C4					113.7(12)
N2−M−N3	85.3(1)	88.0(3)	82.6(1)	82.8(5)	86.3(10)	C5−C6−C7	126.6(2)	126.9(10)	129.6(2)	129(2)	127(2)
N1−M−N4	86.3(1)	88.2(3)	83.5(1)	84.2(4)	85.3(9)	C4−C6−C7					125(2)
N1−M−N3	143.4(1)	161.1(4)	130.4(2)	146.6(5)	135.6(12)	N2−C6−C7	109.1(3)	109.5(10)	110.0(2)	107.2(14)	107(2)
N1−M−N2	89.9(1)	88.8(3)	79.0(1)	87.9(5)	78.9(8)	N2−C9−C8	109.1(3)	109.7(10)	110.4(2)	108.6(13)	114(2)
M−N1−C4	125.9(2)	127.6(7)	101.3(1)	128.1(10)	115.9(11)	C8−C9−C10	125.5(2)	129.4(11)	128.1(2)	127.8(13)	124(2)
M−N1−C1	127.2(2)	124.6(7)	105.5(1)	118.5(12)	124.2(12)	N2−C9−C10	124.5(2)	119.8(10)	121.1(2)	123.4(11)	121(2)
C1−N1−C4	106.7(2)	106.6(8)	106.3(2)	109.8(13)	107.9(12)	C9−C10−C11	113.5(2)	115.0(9)	112.3(2)	114.2(13)	107.5(13)
M−N2−C9	117.5(2)	124.9(6)	104.6(2)	123.3(9)	127.2(13)	N3−C11−C10	123.2(2)	124.4(10)	123.5(2)	118.5(12)	122(2)
M−N2−C6	116.9(2)	127.3(7)	101.4(2)	127.3(9)	115.5(11)	C10−C11−C12	125.9(2)	127.5(11)	124.8(2)	128.3(13)	126.0(14)
C6−N2−C9	106.2(2)	104.9(9)	106.0(2)	107.4(11)	106.0(14)	N3−C11−C12	110.7(2)	108.0(10)	111.3(2)	112.6(12)	112.0(14)
M−N3−C14	120.1(2)	126.4(7)	118.2(2)	131.6(9)	117.3(11)	N3−C14−C13	106.8(2)	109.9(9)	108.0(2)	108.5(12)	108.9(14)
M−N3−C11	128.3(2)	121.8(7)	128.7(2)	125.4(8)	122.8(12)	C13−C14−C16	132.5(2)		123.8(2)		119(2)
C11−N3−C14	107.1(2)	106.8(9)	106.4(2)	103.0(10)	107.7(13)	C13−C14−C15	121.3(2)	126.6(10)	124.5(2)	132.6(13)	124(2)
M−N4−C19	127.0(2)	125.1(7)	127.5(2)	122.8(10)	124.6(11)	N3−C14−C16	111.1(2)		114.5(2)		115.1(13)
M−N4−C16	119.8(2)	127.3(8)	117.3(1)	128.4(9)	117.5(11)	N3−C14−C15	119.7(2)	122.7(9)	119.8(2)	118.6(11)	122(2)
C16−N4−C19	107.1(2)	106.4(9)	106.3(2)	107.4(11)	105.6(12)	C15−C14−C16	59.9(1)		58.8(1)		58.1(11)
N1−C1−C20	121.5(2)	122.9(10)	120.3(2)	128(2)	121.2(13)	C14−C15−C16	60.5(1)	114.0(9)	62.2(1)	117.3(14)	64.2(11)
N1−C1−C2	109.9(2)	108.0(10)	110.4(2)	104(2)	112.6(14)	C14−C16−C15	59.5(1)		59.0(1)		57.7(11)
C2−C1−C20	128.4(2)	128.4(11)	128.5(2)	129(2)	126.1(14)	N4−C16−C15	114.8(2)	124.6(10)	120.0(2)	123.7(14)	122(2)
N1−C4−C3	109.1(2)	108.3(10)	109.9(2)	109(2)	107.6(13)	N4−C16−C14	112.0(2)		112.0(1)		113.6(13)
N1−C4−C5	125.2(2)	123.5(9)	120.4(2)	123.3(12)	119.5(14)	C15−C16−C17	123.3(2)	127.0(11)	126.0(2)	127.2(17)	124.5(13)
N1−C4−C6					115.9(13)	C14−C16−C17	133.3(2)		123.9(2)		120.7(14)
C3−C4−C6					121.9(14)	N4−C16−C17	107.1(2)	108.0(11)	107.9(2)	109(2)	108.9(13)
C3−C4−C5	125.5(2)	126.6(10)	129.3(2)	126(2)	125.4(14)	N4−C19−C18	110.9(2)	110.3(10)	111.2(2)	109(2)	113(2)
C5−C4−C6					59.4(11)	C18−C19−C20	129.5(2)	125.5(11)	124.5(2)	127.8(14)	129.3(14)
C4−C5−C6	116.4(2)	114.3(9)	111.8(2)	110.9(14)	61.2(11)	N4−C19−C20	119.6(2)	124.1(10)	124.2(2)	123.1(13)	118.1(14)
C4−C6−C5					59.4(11)	C1−C20−C19	106.9(2)	113.0(11)	112.3(2)	112(2)	106.8(12)

reduction of **3** using 1 equiv of lithium metal. Such a procedure has been found valuable for producing M(III)−porphyrinogen complexes (M = Co, Cu) *via* a monoelectronic reduction of the corresponding M(II)−monocyclopropaneporphyrinogen compounds.[4] Regardless of the Li/V ratio, however, **3** has always been reduced to the corresponding V(IV)−porphyrinogen complex **5** (Scheme 4).

The synthesis of **5** has been achieved directly from the reaction of the corresponding vanadium(IV) precursor, **4**,[6] and **1** (Scheme 4). The structure of **5** has been assigned according to a large number of structures so far determined[3a,c,4,5b] which have the same peculiarities, including the coordination of lithium cations to the periphery of porphyrinogen (see Experimental Section).

The relative stability of the various oxidation states of a metal gives rise to two general intermolecular redox processes, depending on the coordination environment. They are the oxidation of the complexed ligand by a local excess of the high-valent metal ion, as we found in the case of vanadium, or the oxidation of the local excess of the free ligand by the complexed high-valent metal.

The latter process, occurring in the case of tungsten(VI), allowed us to identify the two- and four-electron oxidized forms of *meso*-octaethylporphyrinogen as their lithium derivatives, respectively reported as **8** and **9B** in Scheme 5.

The complete pathway of W(VI)−porphyrinogen is shown in Scheme 5. Considering the assumption that the redox processes are faster than the complexation of the metal ion by any porphyrinogen form, we can select the preferential formation of one of the species in Scheme 5 by tuning the $WOCl_4$:**1** stoichiometry. This is particularly relevant in the preparation

Table 2. Comparison of Structural Parameters within the M−porphyrinogen Units for Complexes **3** and **7**−**9** (M = V for **3**; M = W for **7** and the Anion of **9**; M = Li1 for **8** and the Cation of **9**)

				9	
	3	**7**	**8**	anion	cation
dist of atoms from the N_4[a] plane (Å)	N1, −0.004(2) N2, 0.004(2) N3, −0.005(2) N4, 0.004(2) V, 0.638(1)	N1, −0.011(10) N2, 0.011(10) N3, −0.011(10) N4, 0.011(10) W, 0.354(2)	N1, −0.010(2) N2, 0.010(2) N3, −0.010(2) N4, 0.010(2) Li1, 0.921(4)	N1, −0.001(15) N2, 0.000(11) N3, −0.001(13) N4, 0.001(12) W, 0.589(1)	N1, −0.001(13) N2, 0.001(13) N3, −0.001(13) N4, 0.001(13) Li1, 0.83(2)
dist of M from A[b] plane (Å)	0.198(1)	0.387(2)	2.096(4)	0.561(1)	1.19(2)
dist of M from B plane (Å)	1.341(1)	0.591(2)	2.154(4)	0.515(1)	1.15(2)
dist of M from C plane (Å)	0.779(1)	0.785(2)	0.897(4)	0.015(1)	1.25(2)
dist of M from D plane (Å)	1.008(1)	0.375(2)	0.959(4)	0.537(1)	1.23(2)
dihedral angle N_4−A (deg)	156.3(1)	156.6(4)	135.1(1)	157.6(5)	124.9(4)
dihedral angle N_4−B (deg)	157.0(1)	151.4(3)	133.9(1)	159.1(4)	125.4(5)
dihedral angle N_4−C (deg)	140.9(1)	162.4(4)	130.2(1)	149.8(6)	124.0(5)
dihedral angle N_4−D (deg)	134.8(1)	167.5(4)	130.0(1)	156.1(6)	124.7(4)
dihedral angle A−C (deg)	117.2(1)	154.7(5)	168.4(1)	129.5(7)	111.1(6)
dihedral angle B−D (deg)	155.6(1)	145.2(5)	169.1(1)	135.2(7)	109.2(5)

[a] N_4 refers to the least-squares mean plane defined by N1, N2, N3, and N4. [b] A−D refer to the least-squares mean planes defined by the pyrrolic rings containing N1, N2, N3, and N4, respectively.

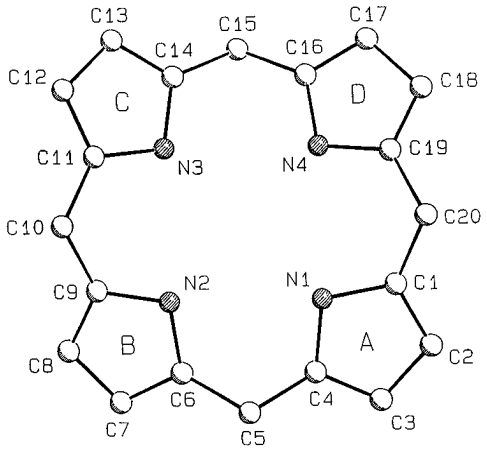

Figure 1. Labeling scheme adopted. In complexes **3** and **8** the cyclopropane unit is formed by the C14, C15, and C16 atoms; in the cation of complex **9** the two cyclopropane units involve the C4, C5, C6 and C14, C15, C16 atoms.

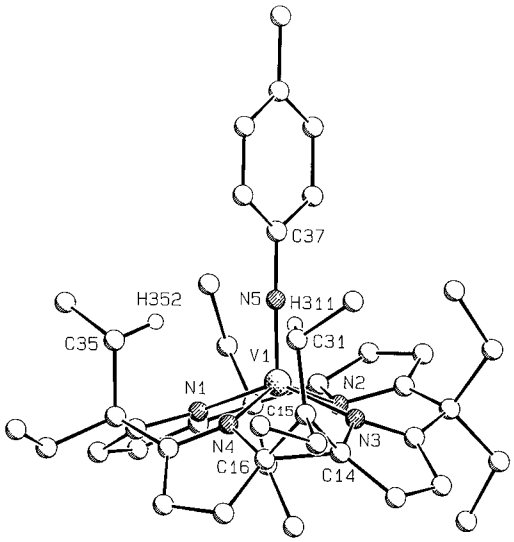

Figure 2. A SCHAKAL perspective view of complex **3**.

of either **8** or **9**, which are the sources of mono(cyclopropane)− and bis(cyclopropane)−porphyrinogen.

After performance of the reaction with a 2:3 molar ratio, **8** can be isolated in a good yield, though its separation from **7** is not always very easy, due to their similar solubilities. Increasing such a ratio up to 4:5 further oxidizes **8** to **9B**, which is the countercation of **9A**. Therefore a mixture of **7** and **9** forms with such a molar ratio. A further increase of the $WOCL_4$:**1** ratio has only some negative consequences, that is, the reaction of **8** or **9** with the excess of the oxide−halide. The impossibility to identify **6**, which is the oxidizing agent of **1** and **8**, is in agreement with the assumption that the redox processes are faster than the complexation of $WOCl_4$ by either **1** or **8**. The bis(cyclopropane) form of porphyrinogen **11** becomes syntheti-

Scheme 3

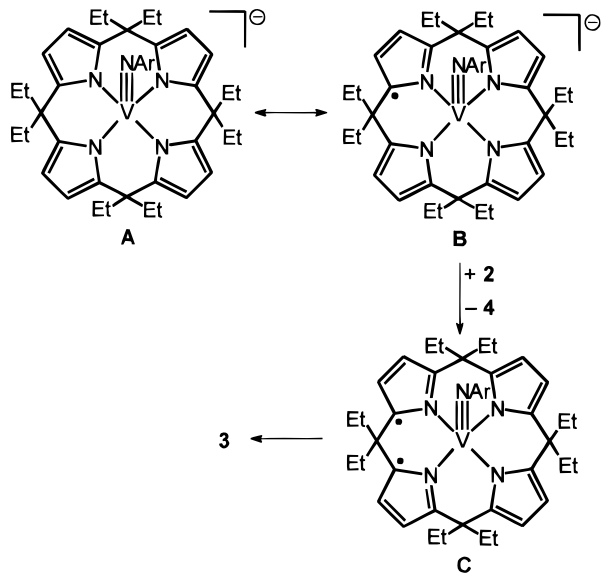

Scheme 4

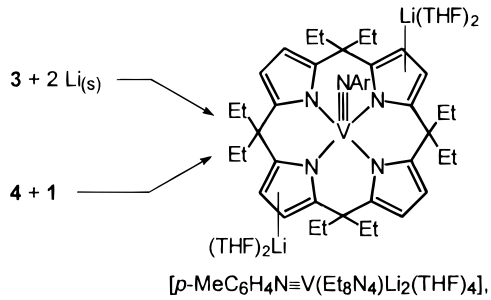

[*p*-MeC$_6$H$_4$N≡V(Et$_8$N$_4$)Li$_2$(THF)$_4$], **5**

Scheme 5

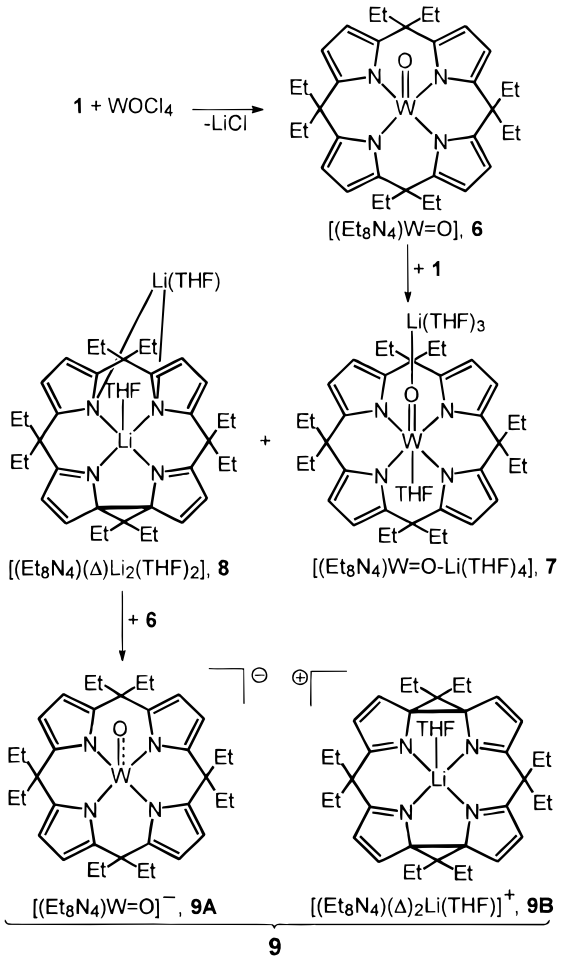

Scheme 6

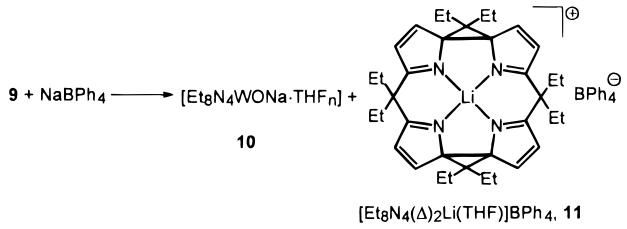

cally available from **9** *via* the cation-exchange reaction shown in Scheme 6 (see Experimental Section).

We can conclude that, with appropriate control of the stoichiometry (2:3 *vs* 4:5), the reaction of $WOCl_4$ with **1** can be used as a preparative method for the isolation of reasonable quantities of **8** and **11**. With the results here reported, we rule out the suspicion that oxidized forms of porphyrinogen exist only as a consequence of transition metal stabilization.[4] Reactions in Scheme 5 are substantially intermolecular electron-transfer processes. The question at this point is *via* which kind of molecular contact does the electron transfer occur? The porphyrinogen periphery binds alkali cations quite strongly, with the lithium cation functioning as a bridge across the porphyrinogen units.[4a,c] This has been clearly shown in the disproportionation of copper(III)−porphyrinogen complexes occurring in hydrocarbons, since the same reaction was reversed upon moving to a THF solution. Scheme 5 is fully supported by the structural determinations of **7**−**9**. These X-ray analyses are crucial, since the paramagnetism of W(V) did not allow an NMR structural inspection in solution of most of the species reported, except for **8** and **11** (*vide infra*).

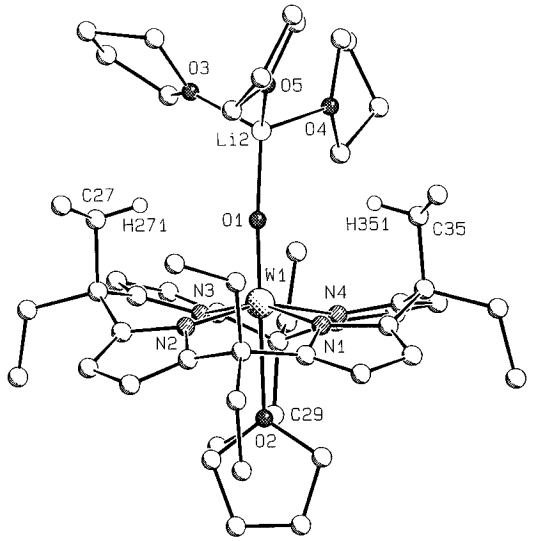

Figure 3. A SCHAKAL perspective view of complex **7**. The disordered atoms are omitted for clarity.

The structure of **7** consists of discrete $[(Et_8N_4)W(THF)OLi(THF)_3]$ molecules (Figure 3). Tungsten exhibits a pseudo-octahedral coordination provided by the four nitrogen atoms of the porphyrinogen ligand in the best equatorial plane; the O1 oxygen atom from the oxo functionality and the O2 oxygen atom from a THF molecule are in axial positions, with the O1−W−O2 angle being 179.6(4)°. The oxo-functionality behaves as an approximately linear bridge, linking a Li cation (called Li2 for sake of comparison with the other complexes) at a normal Li−O distance of 1.90(2) Å and a W1−O1−Li2 angle of 166.6(9)°. The coordination of the Li cation is completed to tetrahedral through the oxygen atoms from three THF molecules, with the $Li-O_{THF}$ distances averaging 1.94(2) Å. The tungsten atom is displaced by 0.354(1) Å from the planar N_4 core toward the O1 oxygen atom at a distance of 1.732(9) Å.[8] The dihedral angle formed by the O2−W−O1 line and the normal to the N_4 core is 2.6(6)°. The W−N bond distances fall in a rather narrow range (Table 1) averaging 2.094(8) Å and are in good agreement with the values of 2.092 and 2.085 Å found in an oxoperoxo(tetraphenylporphyrinato)tungsten(VI)−benzene solvate.[9] The conformation of the ligand is strongly affected by the hexacoordination of the metal, with the ligand assuming an almost flattened, double saddle shape conformation as indicated by the dihedral angles between the N_4 plane and the pyrrole rings and between opposite pyrrole rings (Table 2). In this conformation, the ligand points two hydrogen atoms (H271 and H351) from the C27 and C35 *meso*-methylene carbons symmetrically toward the oxo oxygen [C27···O1, 3.44(2) Å; H271···O1, 2.54 Å; C27−H271···O1, 153°; C35···O1, 3.45(2) Å; H351···O1, 2.54 Å; C35-H351···O1, 156°]. On the opposite side, a significant contact involves the C29 methylene carbon and the O2 oxygen atom [C29···O2, 3.354(14) Å; H291···O2, 2.44 Å; C29−H291···O2, 158°]. Bond distances and angles within the macrocyclic ligand are in agreement with some π delocalization within the pyrrole rings.

The structure of **8** consists of discrete neutral molecules of formula $[Et_8N_4(\Delta)Li_2(THF)_2]$ (Figure 4). Two Li cations are bonded to the dianionic ligand on opposite sides with respect to the N_4 core. The former, Li1, is σ-bonded to the four nitrogen atoms, while the latter, Li2, is σ-bonded only to the negatively

(8) Nugent, W. A.; Mayer, J. M. *Metal-Ligand Multiple Bonds*; Wiley: New York, 1988; p 153 and references therein.

(9) Yang, C.-H.; Dzugan, S. J.; Goedken, V. L. *J Chem. Soc., Chem. Commun.* **1985**, 1425.

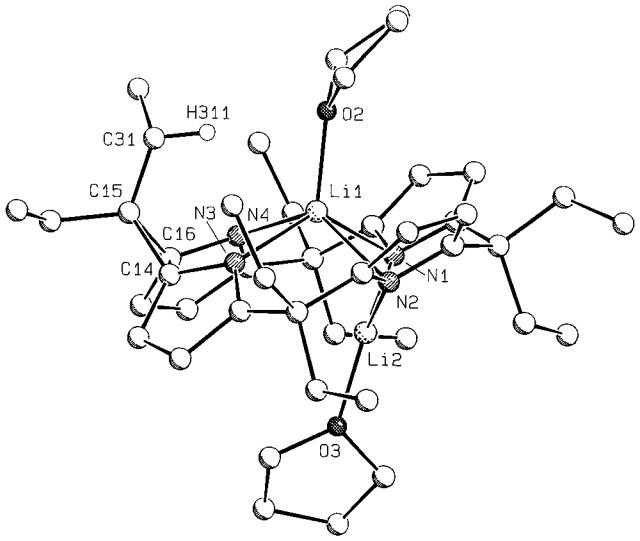

Figure 4. A SCHAKAL perspective view of complex **8**.

charged N1 and N2 nitrogen atoms. Li1 is five-coordinate, while Li2 is in a trigonal planar coordination. In both cases, coordination is completed by an oxygen atom from a THF molecule [O2 and O3 for Li1 and Li2, respectively). The N_4 core shows small, but significant, tetrahedral distortions with Li1 and Li2 lying at 0.921(4) and −1.281(4) Å from it. The direction of the Li−O2 line is perpendicular to the N_4 plane, the dihedral angle that it forms with the normal to that plane being 1.3(1)°. The conformation of the macrocycle is different from those previously observed for porphyrinogen complexes containing a cyclopropane unit,[4] the pair of rings (C and D) bridged by one cyclopropane unit being tilted down and the other two (A and B) being tilted up with reference to the N_4 plane, so that opposing rings turn out to be approximately parallel, although not coplanar (Table 2). The upward bending of the two A and B rings makes room to accommodate the Li2 cation, and the asymmetry of the Li−porphyrinogen interactions could be related to the asymmetry of the charge distribution on the dianionic ligand resulting from cyclopropane formation. The dihedral angle between the cyclopropane unit and the N_4 core is 133.3(1)°. The C and D rings bridged by the cyclopropane unit have lost some aromatic character, each one showing a system of conjugated double bonds as indicated by the double-bond character of the N3−C11, C12−C13, N4−C19, and C17−C18 bond distances and the single-bond character of all of the others (N3−C14, C11−C12, C13−C14, N4−C16, C16−C17, C18−C19). The configurations at the C14 and C16 asymmetric carbon atoms are *S* and *R*, respectively, with reference to the coordinates of Table S3. Since the space group is centrosymmetric, the enantiomeric diastereoisomer is present in the structure (Figure 4). The ^{1}H NMR spectrum of complex **8** at room temperature revealed a certain degree of fluxionality. The spectrum is resolved by cooling the sample to 273 K. Two pairs of doublets are then seen for the pyrrole moiety, one at 6.8 and 6.5 ppm (J = 4.8 Hz) and the other at 6.45 and 6.35 ppm (J = 2.4 Hz). The aliphatic region shows the presence of a particularly shielded CH_2 group (1.6 *vs* 2.15 ppm in **1** and 2.02 ppm for the lowest CH_2 in complex **11**) and of a particularly deshielded CH_3 (1.43 *vs* 1.09 ppm in **1** and 1.1 ppm for the highest value in **10**). Further cooling of the sample did not cause notable variation, but there was signal broadening below −20 °C.

In complex **9** the ion-pair structure of **7** has been converted into the ion-separated form due to the complexation of lithium cation by the bis(cyclopropane)−porphyrinogen; thus the structure of **9** consists of discrete $[(Et_8N_4)WO]^-$ anions (Figure 5)

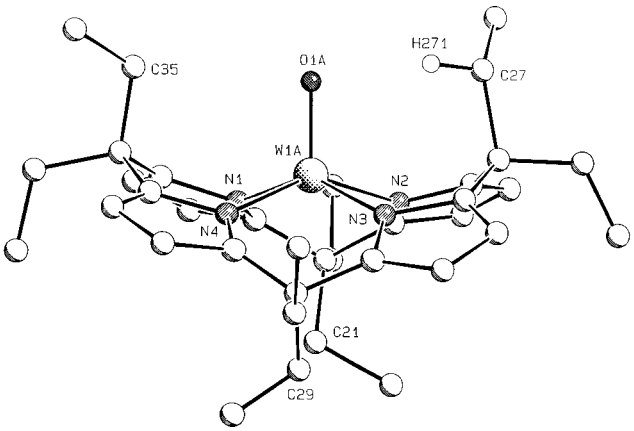

Figure 5. A SCHAKAL perspective view of the anion in complex **9**. The disordered atoms are omitted for clarity.

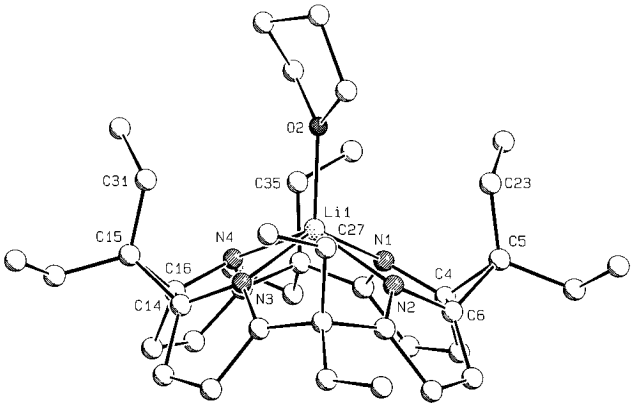

Figure 6. A SCHAKAL perspective view of the cation in complex **9**. The disordered atoms are omitted for clarity.

and $[Et_8N_4(\Delta)_2Li(THF)]^+$ cations (Figure 6) separated by van der Waals interactions. In the anion, a tungstenyl moiety is bound to the four nitrogen atoms of the tetraanionic porphyrinogen ligand, with tungsten exhibiting a square pyramidal coordination. In one direction, the W−O1 bond [1.699(1) Å][8] forms a dihedral angle of 1.9(4)° with the normal to the N_4 core. The W−N bond distances fall in a rather narrow range (Table 1), averaging 2.052(6) Å. This value is significantly shorter than that found in complex **7**. The ligand assumes an almost regular, double saddle-shaped conformation, as indicated by the dihedral angles between the N_4 plane and the pyrrole rings and those between opposite pyrrole rings (Table 2). The presence of the oxo functionality determines a remarkable out-of-plane displacement of the metal from the planar N_4 core (Table 2) and a consequent distortion of the ligand emphasized by the difference in the C···C separation for the *meso*-methylene carbons positioned below (C21, C29) and above (C27, C35) the coordination plane, with the C21···C29 and C27···C35 distances being 4.78(4) and 6.19(3) Å (Figure 5). The role of the *meso*-ethyl groups remains an essential characteristic of the present ligand. Significantly close contacts have been observed between the C27 and C35 methylene carbons and the oxo functionality [C27···O1A, 3.09(2) Å; H271···O1A, 2.24 Å; C27-H271···O1A, 145°; C35···O1A, 3.12(3) Å. Hydrogens bonded to C35 have been ignored because of the disorder involving the attached C36 methyl. Such close contacts mimic a possible transition state in the mechanism of oxo transfer to unactivated C−H bonds.[10]

In **9B**, a $Li(THF)^+$ unit is σ-bonded to the four nitrogen atoms of the neutral porphyrinogen molecule containing two cyclo-

(10) Hill, C. L. In *Activation of Functionalization of Alkanes*; Hill, C. L., Ed.; Wiley: New York, 1989; p 243.

Table 3. Experimental Data for the X-ray Diffraction Studies on Crystalline Complexes **3** and **7**−**9**

	compound			
	3	**7**	**8**	**9**
chem formula	$C_{43}H_{55}N_5V$	$C_{52}H_{80}LiN_4O_5W$	$C_{44}H_{64}Li_2N_4O_2$	$C_{36}H_{48}N_4OW$
a (Å)	11.202(2)	12.032(4)	11.250(1)	12.199(2)
b (Å)	17.290(3)	20.765(5)	19.317(2)	25.580(5)
c (Å)	11.112(2)	11.841(4)	19.080(2)	22.320(4)
α (deg)	107.30(2)	97.39(3)	90	90
β (deg)	108.12(2)	119.19(2)	100.80(1)	90
γ (deg)	96.91(2)	89.92(3)	90	90
V (Å^3)	1898.5(7)	2554.8(15)	4073.0(7)	6965(2)
Z	2	2	4	4
fw	692.9	1032.0	694.9	1352.5
space group	$P\bar{1}$ (No. 2)	$P\bar{1}$ (No. 2)	$P2_1/c$ (No. 14)	$P2_12_12_1$ (No. 19)
t (°C)	22	22	22	22
λ (Å)	1.541 78	0.710 69	1.541 78	0.710 69
ρ_{calcd} (g cm^{-3})	1.212	1.342	1.133	1.290
μ (cm^{-1})	24.56	23.54	4.92	17.42
transm coeff	0.903−1.000	0.721−1.000	0.939−1.000	0.798−1.000
R[b]	0.052	0.056	0.046	0.058 [0.071][a]
w*R*2[b]	0.136	0.118	0.119	0.129 [0.159]

[a] Values in brackets refer to the inverted structure. [b] $R = \sum|\Delta F|/\sum|F_o|$ calculated for the unique observed data. [c] $wR2 = [\sum(w(\Delta F^2)^2/\sum(wF_o^2)^2]^{1/2}$ calculated for the unique observed data.

propane moieties. The formation of these units causes a completely different conformation as compared to complex **8**. The four pyrrole rings are bent in the same direction with respect to the N_4 core. The bending is almost the same, as seen from the values of the dihedral angles (Table 2). This gives rise to a cavity having a cone section conformation similar to that previously observed in the Fe and Co derivatives[3c,4a,b] and to that seen in calix[4]arenes.[11] This conformation leads the four methylene carbons (C23, C27, C31, C35) to be arranged above the coordination plane to give four rather long contacts with the O2 oxygen atom: O2···C23, 3.55(3), O2···C31, 3.57(3), O2···C27, 3.98(2), O2···C35, 4.03(2) Å. The C27···C35 and C23···C31 separations [7.22(2) and 6.77(2) Å, respectively] are in good agreement with the corresponding ones for the cation $[Et_8N_4(\Delta)_2Fe(Cl)]^+$ of the iron derivative.[4b] The more symmetric arrangement of the four methylene carbons in the cation $[Et_8N_4(\Delta)_2Co(Cl)]^+$ [C···C separations of 6.99(2) and 6.95(2) Å] is related to the presence of the $Cu_4Cl_5^-$ anion intimately bound to the pyrrole rings.[4b] So, the cone section, calix-type conformation could be considered the result of the formation of two cyclopropane units rather than the result of intramolecular contacts involving a fifth ligand. The Li cation is strongly displaced from the planar N_4 core (Figure 6) exhibiting a pyramidal coordination (Table 3). In the direction of the Li−O2 bond, a dihedral angle of 1.7(8)° is formed with the normal to the N_4 plane. The Li−N bond distances are in good agreement with the Li1−N3 and Li−N4 bond distances of complex **8** involving uncharged nitrogens (Table 1). Bond distances and angles within the ligand are consistent with a system of conjugated double bonds in the four pyrrole rings as a consequence of the formation of the two cyclopropane units and as indicated by the double-bond character of the N1−C1, C2−C3, N2−C9, C7−C8, N3−C11, C12−C13, N4−C19, and C17−C18 bonds and by the single-bond character of all of the other bonds. A solution structural information on cation **9B** derives from our NMR studies on **11**. Inspection of the ^{1}H NMR of complex **11** at room temperature reveals that the molecule is highly symmetric in solution showing a pair of doublets (7.41 and 6.645 ppm) for the pyrrole protons and four different methylene quartets and methyl triplets. The methylene region spans over 0.5 ppm (δ = 2.5-2.0) whereas the methyls resonance are more grouped together (δ = 1.1−0.8). The coupling constants for the pyrrole protons (J = 4 Hz) reveals the diene character of the system being higher than those normally found for the pyrrole moiety. The coupling constants of the ethyl groups (J = 7 Hz) fall inside the typical values for free rotating systems.

Scheme 7

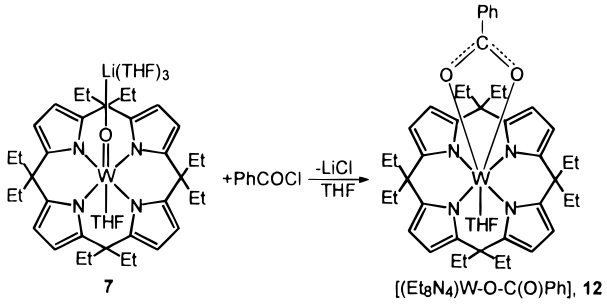

It is quite difficult to assess from the structural parameters the localization of the negative charge in **7** and **9A**, since the W−O distance maintains a high degree of double-bond character. This fact suggests a preferable localization of the charge on the porphyrinogen moiety, even though we observed an unusual Li^+ binding by the electron-rich tungstenyl unit. The oxo group remains the preferred site of reactivity with electrophiles, as exemplified in Scheme 7 for the reactivity of **7** with benzoyl chloride.

Complex **12** is the inorganic analogue of an ester. A strong C−O band at 1602 cm^{-1} is present, which can indicate a bidentate bonding mode of the ester unit to the metal.

Conclusions

The reaction of high-valent early transition metals, *i.e.* vanadium(V) and tungsten(VI), with the *meso*-octaethylporphyrinogen tetraanion allowed us to discover two different redox processes: (i) the oxidation of porphyrinogen complexes by high-valent metal halides; (ii) the oxidation of the porphyrinogen−lithium derivatives by porphyrinogen−metal complexes. In the latter case, we were able to tune these reactions to obtain a reasonable synthetic method for the oxidized forms of porphyrinogen containing either mono- or bis(cyclopropane) units. This finding was particularly relevant for showing that oxidized forms of porphyrinogen do not need to be bound to a

(11) Corazza, G.; Floriani, C.; Chiesi-Villa, A.; Guastini, C. *J. Chem. Soc., Chem. Commun.* **1990**, 640. Corazza, G.; Floriani, C.; Chiesi-Villa, A.; Rizzoli, C. *Inorg. Chem.* **1991**, *30*, 4465.

transition metal and that oxidized forms of porphyrinogen become available as ligands in coordination chemistry, promising a peculiar redox chemistry associated with the easy cleavage of the cyclopropane moiety.

Experimental Section

All operations were carried out under an atmosphere of purified nitrogen. All solvents were purified by standard methods and freshly distilled prior to use. NMR spectra (δ) were recorded on a 200-AC and on a 400-DPX Bruker instruments.

Synthesis of 3. **2** (10.25 g, 39.09 mmol) was suspended in 200 mL of diethyl ether with the presumed immediate formation of an orange etherate adduct. The resulting supension was then cooled to −78 °C, and **1** (16.63 g, 19.5 mmol) was added in portions. An immediate reaction ensued with the formation of a red suspension, and the mixture was allowed to warm to room temperature and stir overnight. The resulting suspension was then transferred into an extractor and the solid extracted with the reaction solvent at reflux for 24 h. A bright red suspension resulted, and the red solid was collected on a filter and dried under vacuum (63% yield). Anal. Calcd for $C_{43}H_{55}N_5V$: C, 74.5; H, 7.95; N, 10.11. Found: C, 74.1; H, 8.39; N, 9.86. IR (selected peaks, cm^{-1}): 3073 (s, s); 1562 (s, s); 1321 (s, s); 1243 (s, s); 1065 (s, s); 962 (m, s); 815 (s, s). $\mu_{295} = 1.81\ \mu_B$.

Synthesis of 5. Method A. Sodium sand (0.112 g, 4.87 mmol) was added to an orange-red solution of **2** (1.418 g, 5.41 mmol) in THF (80 mL), which was cooled to −40 °C. The reaction mixture was stirred at −20 °C for 48 h. A reddish solution resulted with a small quantity of a pale solid, and all the Na was consumed. The solvent was then evaporated under reduced pressure, and diethyl ether (70 mL) was added to the residue. The resulting red suspension was cooled to −50 °C, and **1** (4.26 g, 5.00 mmol) was added in portions. The reaction mixture was warmed to room temperature and stirred overnight. A reddish suspension resulted which was transferred into an extractor and the solid extracted at reflux for 16 h. The resulting suspension was cooled to room temperature and stored for 12 h at 4 °C. A yellow amber microcrystalline solid was collected on a filter and dried in vacuo (75%). Anal. Calcd for **5**, $C_{59}H_{87}Li_2N_5O_4V$: C, 71.24; H, 8.75; N, 7.04. Found: C, 71.38; H, 8.66; N, 6.82. IR (selected values, cm^{-1}): 1490 (m, s); 1327 (m, s); 1260 (m, s); 1150 (m, s); 1066 (s, b); 1033 (M, s); 921 (w, s); 887 (w, s); 820 (s, s); 760 (s, s).

Method B. Li (sand) (0.053 g, 7.64 mmol) was added in one portion to a solution of **3** (2.006 g, 2.90 mmol) in THF (80 mL). The reaction mixture was stirred at room temperature for 48 h. The solvent was then evaporated under reduced pressure, and diethyl ether (60 mL) was added to the residue. This suspension was filtered into an extractor and extracted at reflux for 2 h. The resulting suspension was cooled to room temperature and stored at 4 °C overnight. A yellow microcrystalline solid was collected on a filter and dried under vacuum (70%). The analytical results are identical to those reported above.

Synthesis of 7 + 8. $WOCl_4$ (2.46 g, 7.21 mmol) was added in one portion to a cold (−70 °C) solution of **1** (9.60 g, 11.25 mmol) in THF (120 mL). The reaction mixture was allowed to warm to room temperature, and the resulting purple solution was stirred overnight. The solvent was evaporated under reduced pressure, and 100 mL of diethyl ether was added. The resulting suspension was transferred into an extractor and the solid residue extracted at reflux for 2 h. A white insoluble solid (LiCl) was left on the filter, and upon standing, orange **8** crystallized from the solution. Crystals suitable for X-ray diffraction were grown by cooling a saturated solution in diethyl ether to 4 °C. The solid was then collected and dried in vacuum (58%). Anal. Calcd for **8**, $C_{44}H_{64}Li_2N_4O_2$: C, 76.1; H, 9.22; N, 8.07. Found: C, 74.98; H, 9.26, N, 8.10. ^{1}H NMR (400 MHz, C_7D_8, 273 K): 0.65 (m, 6 H, CH_3); 0.86 (t, 6 H, CH_3, $J = 7$ Hz); 0.97 (m, 9 H, CH_3); 1.32 (bs, 8 H, THF); 1.42 (t, 3 H, CH_3, $J = 7$ Hz); 1.61 (q, 2 H, CH_2, $J = 7$ Hz); 1.86 (m, 4 H, CH_2); 2.00 (q, 2 H, CH_2, $J = 7$ Hz); 2.05 (m, 2 H, CH_2═$C_6D_5CD_3$), 2.2 (q, 2 H, CH_2, $J = 7$ Hz); 2.51 (m, 4 H, CH_2); 6.35 (d, 2 H, Py, $J = 2.8$ Hz); 6.44 (d, 2 H, Py, $J = 2.4$ Hz); 6.49 (d, 2 H, Py, $J = 4.8$ Hz); 6.85 (d, 2 H, Py, $J = 4.8$ Hz). IR (selected values, cm^{-1}): 3091 (m, s); 1573 (s, s); 1317 (w, s); 1264 (w, s); 1046 (s, s); 912 (m, s); 792 (m, s); 730 (m, s). The mother liquors were concentrated under reduced pressure to 25 mL, and purple gray microcrystalline **7** crystallized (74%).

Synthesis of 7 + 9. Method A. **1** (10.54 g, 12.36 mmol) was added in portions to a cold (−40 °C) solution of $WOCl_4$ (4.28 g; 12.54 mmol) in THF (150 mL). The mixture was warmed to room temperature, and the resulting purple solution was stirred overnight. The solvent was then evaporated under reduced pressure, and diethyl ether (80 mL) was added. A purple suspension resulted which was transferred into an extractor and the solid extracted at reflux for 3 h. A purple suspension was obtained from the extraction, while a pink solid was left on the extractor. The purple suspension was cooled to room temperature and stored at 4 °C for 12 h. A purple-gray solid was then collected on a filter and dried in vacuo (41%). Anal. Calcd for **7**, $C_{52}LiH_{80}N_4O_5W$: C, 60.52; H, 7.76; N, 5.46. Found: C, 59.73; H, 7.70; N, 5.54. IR (selected values, cm^{-1}): 1612 (w, b); 1573 (w, s); 1321 (s, s); 1237 (s, s); 1138 (s, s); 1070 (s, s); 951 (s, s); 863 (m, s). $\mu_{295} = 1.74\ \mu_B$. The pink residue was dissolved in THF (50 mL), and LiCl was precipitated by addition of toluene (70 mL) and filtered off after standing 3 h at room temperature. Concentration of the resulting solution to 30 mL caused precipitation of a pink microcrystalline solid, which was collected on a filter and dried under vacuum (54%). Anal. Calcd for **9**, $C_{76}H_{96}LiN_8O_2W$: C, 67.9; H, 7.20; N, 8.33. Found: C, 67.78; H, 8.05, N, 8.34. IR (selected values, cm^{-1}): 1569 (m, s); 1365 (m, s); 1317 (w, s); 1239 (w, s); 1077 (s, s); 972 (s, s); 758 (s, s).

Method B. **1** (14.39 g, 16.87 mmol) was added in portions to a cold (−40 °C) solution of $WOCl_4$ (4.57 g, 13.37 mmol) in THF (150 mL). The mixture was warmed to room temperature, and the resulting purple solution was stirred overnight. The solvent was then evaporated under reduced pressure, and diethyl ether (80 mL) was added. A purple suspension resulted which was transferred into an extractor and the solid extracted at reflux for 3 h. A purple suspension resulted from the extraction, and a pink solid was left on the extractor. The purple suspension was cooled back to room temperature and stored at 4 °C for 12 h. The solid was then collected on a filter and dried in vacuo (66%). Anal. Calcd for **7**, $C_{52}H_{80}LiN_4O_4W$: C, 60.52; H 7.76; N, 5.46. Found: C, 59.73; H, 7.70; N, 5.54. IR (selected values, cm^{-1}): 1612 (w, b); 1573 (w, s); 1321 (s, s); 1237 (s, s); 1138 (s, s); 1070 (s, s); 951 (s, s); 863 (m, s). $\mu_{295} = 1.74\ \mu_B$. The pink residue was dissolved in THF (50 mL), and LiCl was precipitated by addition of toluene (70 mL) and filtered off after standing 3 h at room temperature. Concentration of the resulting solution to 30 mL caused precipitation of a pink microcrystalline, which was collected on a filter and dried under vacuum (47%). Anal. Calcd for **9**, $C_{76}H_{96}LiN_8O_2W$: C, 67.90; H, 7.20; N, 8.33. Found: C, 67.78; H, 8.05; N, 8.34. IR (selected values, cm^{-1}): 1569 (m, s); 1365 (m, s); 1317 (w, s); 1239 (w, s); 1077 (s, s); 972 (s, s); 758 (s, s).

Synthesis of 11. **9** (1.59 g, 1.18 mmol) was dissolved in DME (70 mL), and degassed $NaBPh_4$ (0.403 g, 1.18 mmol) was added in one portion. The resulting purple solution was stirrred overnight and the solvent evaporated under reduced pressure. Diethyl ether (70 mL) was then added to the residue and the resulting purple suspension transferred into an extractor and extracted at reflux with the mother liquor. A white residue was left on the extractor which was dried under vacuum (75%). Anal. Calcd for **11**, $C_{60}H_{68}BN_4Li$: C, 81.98; H, 7.80; N, 6.37. Found: C, 81.55; H, 7.81; N, 6.29. ^{1}H NMR (400 MHz, C_6D_6, 298 K): 0.816 (t, 6 H, CH_3, $J = 7$ Hz); 0.88 (m, 12 H, CH_3); 1.07 (m, 6 H, CH_3, $J = 7$ Hz); 2.04 (q, 4 H, CH_2, $J = 7$ Hz), 2.18 (q, 4 H, CH_2, $J = 7$ Hz); 2.4 (q, 4 H, CH_2, $J = 7$ Hz); 2.55 (q, 4 H, CH_2, $J = 7$ Hz); 6.6 (d, 4 H, Py, $J = 4$ Hz); 6.9 (t, 4 H, BPh_4, $J = 7$ Hz); 7.05 (t, 8 H, BPh_4, $J = 8$ Hz); 7.35 (m, 8 H, BPh_4); 7.40 (d, 4 H, CH_2, $J = 4$ Hz).

Synthesis of 12. Benzoyl chloride (0.285 g, 2.03 mmol) was added via syringe to a solution of **7** (2.08 g, 2.03 mmol) in THF (70 mL). The resulting solution was stirred at room temperature for 48 h. The solvent was then evaporated under reduced pressure and diethyl ether (50 mL) added. The resulting purple suspension with a pale solid was filtered and the product crystallized from the filtrate (1.045 g). Anal. Calcd for **12**·2THF, $C_{55}H_{77}N_4O_5W$: C, 62.43; H, 7.34; N, 5.30. Found: C, 62.34; H, 7.60; N, 5.38. IR (selected values, cm^{-1}): 1602 (vs, s); 1544 (m, s); 1375 (s, s); 1318 (s, s); 1273 (s, s); 1247 (s, s); 1132 (m, s); 1074 (s, s); 953 (s, s); 881(s, s); 757 (s, s).

X-ray Crystallography for Complexes 3 and 7−9. Suitable crystals were mounted in glass capillaries and sealed under nitrogen.

The reduced cells were obtained with use of TRACER.[12] Crystal data and details associated with data collection are given in Tables 3 and S1. Data were collected at room temperature (295 K) on a single-crystal diffractometer (Siemens AED for **3** and **8**, Rigaku AFC6S for **7**, and Enraf-Nonius CAD4 for **9**). For intensities and background, the individual reflection profiles were analyzed.[13] The structure amplitudes were obtained after the usual Lorentz and polarization corrections,[14] and the absolute scale was established by the Wilson method.[15] The crystal quality was tested by ψ scans showing that crystal absorption effects could not be neglected for complexes **3**, **7**, and **9**. Data were then corrected for absorption using ABSORB[16] for **3** and a semiempirical method for **7** and **9**.[17] The function minimized during the least-squares refinement was $\Delta w(\Delta F^2)^2$. Anomalous scattering corrections were included in all of the structure factor calculations.[18b] Scattering factors for neutral atoms were taken from ref 18a for non-hydrogen atoms and from ref 19 for H. Structure solutions and refinements were based on the observed reflections [$I > 2\sigma(I)$]. The structures were solved by the heavy atom method starting from a three-dimensional Patterson map for **3**, **7**, and **9** and by using SHELX86[20] for **8**. Refinements were done by full-matrix least-squares, first isotropically and then anisotropically for all the non-H atoms, except for some disordered atoms. In the last stage of the refinements, the weighting scheme $w = 1/[\sigma^2(F_o^2) + (aP)^2]$ (with $P = (F_o^2 + 2F_c^2)/3$ and $a = 0.1122$, 0.0472, 0.0790, and 0.0435 for **3**, **7**, **8**, and **9**, respectively) was applied. All calculations were performed by using SHELX76[21] for the early stages of solution and SHELXL92[22] for the refinement. The final difference maps showed no unusual feature, with no significant peak above the general background except for the residual peaks of 0.89 in **3** and 1.30 e Å^{-3} in **7** midway along the V−N5 and W−O1 bonds, respectively.

Complex 3. The structure was refined in a straightforward manner. The H atoms were located from difference Fourier maps and introduced in the subsequent refinements as fixed atom contributions with isotropic *U*'s fixed at 0.08 Å^2.

Complex 7. The three THF molecules bonded to the lithium cation were affected by high thermal parameters indicating the presence of disorder, which was solved by splitting the the C42, C43, C44, C47, C48, C51, and C52 atoms over two positions (A and B) and isotropically refined with a site occupation factor of 0.5. Except for those related to the disordered atoms, which were ignored, the H atoms were located from difference Fourier maps and introduced in the subsequent refinements as fixed atom contributions with isotropic *U*'s fixed at 0.10 Å^2.

Complex 8. The structure refinement was straightforward. The H atoms related to the porphyrinogen molecule were located from difference Fourier maps; those associated with the THF molecules were put in geometrically calculated positions. All the hydrogen atoms were introduced in the subsequent refinements as fixed atom contributions with isotropic *U*'s fixed at 0.08 Å^2.

Complex 9. In the anion, the tungstenyl moiety was found to be affected by a severe disorder. This was solved by splitting the W1 and O1 atoms over two positions (A and B) symmetrically arranged above and below the N_4 core of the porphyrinogen ligand with a site occupation factor at first deduced from the height of the peaks on a ΔF map. Refinement was done first isotropically and then anisotropically for W1 (A and B) and O1A allowing the site occupation factor (sof) to vary. At the end of the refinement, the value of the sof converged to 0.876(2) for the A position [0.124(2) for B].

The disorder of the WO moiety implies a disorder of the whole molecule, as clearly indicated by the rather high values reached by the U_{ij} thermal parameters of the pyrrole peripheral carbon atoms and of the C21, C27, C29, and C35 methylene carbon atoms approaching the disordered oxo oxygen above and below the N_4 core. Any attempt to solve the disorder in terms of partial atoms was unsuccessful probably due to the low percentage of the B position. So, the anisotropic model was considered satisfactory in spite of the resulting poor accuracy of the structural parameters of the anion.

As it usually happens, some methyl carbon atoms (C22 and C36 for the anion, C26 for the cation) and the THF molecule (C41···C44) bonded to the Li cation were affected by high thermal motion (or disorder), with their thermal parameters reaching unacceptably high values. The best fit was found considering all these atoms statistically distributed over two positions (A and B) isotropically refined with a site occupation factor of 0.5. During the refinement, a constraint was applied to the THF molecule, the C−O and C−C bond distances being fixed to 1.48(1) and 1.54(1) Å, respectively. All the H atoms except those associated with the disordered atoms, which were ignored, were put in geometrically calculated positions and introduced in the subsequent refinements as fixed atom contributions with isotropic *U*'s fixed at 0.12 Å^2. Since the space group is polar, the crystal chirality was tested by inverting all the coordinates ($x, y, z \rightarrow -x, -y, -z$) and refining to convergence once again. The resulting *R* values quoted in Table 3 indicated that the original choice should be considered the correct one.

Final atomic coordinates are listed in Tables S2−S5 for non-H atoms and in Tables S6−S9 for hydrogens. Thermal parameters are given in Tables S10−S13, and bond distances and angles, in Tables S14−S17.[23]

Acknowledgment. We thank the Fonds National Suisse de la Recherche Scientifique (Grant No. 20-40268.94) for financial support.

Supporting Information Available: ORTEP drawing (Figures S1−S5) and tables giving crystal data and details of the structure determination, fractional atomic coordinates, anisotropic thermal parameters, bond lengths, and bond angles for **3** and **7**−**9** (35 pages). This material is contained in many libraries on microfiche, immediately follows this article in the microfilm version of the journal, can be ordered from the ACS, and can be downloaded from the Internet; see any current masthead page for ordering information and Internet access instructions.

JA9543309

(12) Lawton, S. L.; Jacobson, R. A. *TRACER, a cell reduction program*; Ames Laboratory, Iowa State University of Science and Technology: Ames, IA, 1965.

(13) Lehmann, M. S.; Larsen, F. K. *Acta Crystallogr., Sect. A: Cryst. Phys., Diffr., Theor. Gen. Crystallogr.* **1974**, *A30*, 580.

(14) Data reduction, structure solution, and refinement were carried out on an ENCORE 91 computer and on an IBM AT personal computer equipped with an INMOS T88 transputer.

(15) Wilson, A. J. C. *Nature* **1942**, *150*, 151.

(16) Ugozzoli, F. *Comput. Chem.* **1987**, *11*, 109.

(17) North, A. C. T.; Phillips, D. C. Mathews, F. S. *Acta Crystallogr., Sect. A: Cryst. Phys., Diffr., Theor. Gen. Crystallogr.* **1968**, *A24*, 351.

(18) (a) *International Tables for X-ray Crystallography*; Kynoch Press: Birmingham, England, 1974; Vol. IV, p 99. (b) Ibid., p 149.

(19) Stewart, R. F.; Davidson, E. R.; Simpson, W. T. *J. Chem. Phys.* **1965**, *42*, 3175.

(20) Sheldrick, G. *SHELX86: Program for the solution of Crystal Structure from Diffraction Data*; University of Göttingen: Göttingen, Germany, 1986.

(21) Sheldrick, G. M. *SHELX76: Program for Crystal Structure Determination*; University of Cambridge: Cambridge, England, 1976.

(22) Sheldrick, G. M. *SHELXL92: Program for Crystal Structure Refinement*; University of Göttingen: Göttingen, Germany, 1992.

(23) See paragraph at the end of paper regarding Supporting Information.